Supporting Information

Agarwal et al. 10.1073/pnas.1114224109

SI Materials and Methods

Crystallization of MccF and Ligand Complexes. Crystallization of the apo MccF and all variants was carried out using the hanging drop vapor diffusion technique. Typically, 1 μL of the protein (9 mg/mL in 20 mM Hepes, 100 mM KCl, pH 7.5) was added to 1 μL of precipitant (either 12% PEG 20,000, 0.1 M MES, pH 6.5 or 10% PEG 8,000, 8% ethylene glycol, 0.1 M Hepes, pH 7.5) and equilibrated against the same solution at 9 °C. Selenomethionine-incorporated MccF was crystallized under similar conditions. Complex with microcin C7 (McC7), aspartyl sulfamoyl adenylate (DSA), or glutamyl sulfamoyl adenylate (ESA) were generated by soaking apo crystals with 5 mM final concentration of substrate compounds added to the precipitant for 12 h. Crystals were vitrified by soaking in precipitant supplemented with 30% ethylene glycol prior to direct immersion in liquid nitrogen.

X-Ray Crystallographic Data Collection and Structure Determination. Initial crystallographic phases were determined solved by single wavelength anomalous diffraction utilizing anomalous scattering from the five selenium-substituted methionine residues per monomer of MccF. A fourfold redundant dataset was collected from crystals of selenomethionine-incorporated MccF at the selenium absorption edge, to a limiting resolution of 1.45 Å (overall $R_{\text{merge}} = 7.2$, $I/\sigma(I) = 13.7$ in the highest resolution shell) utilizing a Mar 300 CCD detector (Life Sciences Collaborative Access Team, Sector 21 ID-D, Advanced Photon Source). Data were indexed and scaled using the HKL2000 package (1). Selenium sites were identified and refined for phase calculation using HySS (2), yielding an initial figure of merit of 0.439 (acentric/centric = 0.454/0.137) to 1.45-Å resolution. The resultant electron density map was of exceptional quality and permitted most of the main-chain and 50% of side-chain residues to be automatically built using phenix autobuild (3). The remainder of the model was fitted using Coot (4) and further improved by rounds of refinement with REFMAC5 (5) and manual building. Subsequent rounds of model-building and crystallographic refinement utilized data from a native crystal of MccF grown under similar conditions that diffracted to 1.30-Å resolution (overall $R_{\text{merge}} = 6.5$, $I/\sigma(I) = 6.7$ in the highest resolution shell). Cross-validation, using 5% of the data for the calculation of the free R factor, was utilized throughout the model-building process in order to monitor building bias (6).

The crystal structures of MccF mutants S118A, N220A/K247A/S118A, and W186F in complex with AMP were determined to resolutions of 1.5, 1.7, and 1.5 Å, respectively, and MccF-S118A cocrystal structures with DSA, ESA, and processed McC7 to resolutions of 1.5, 1.3, and 1.3 Å, respectively, were determined by molecular replacement using the coordinates of native MccF as a search probe. Each of the structures was refined and validated using the procedures detailed above. For each of the structures, the stereochemistry of the model was monitored throughout the course of refinement using PROCHECK (7).

MccF Enzyme Kinetics. Kinetics for cleavage of ESA by MccF was monitored by coupling the glutamate production to reduced NADH generation by bovine glutamate dehydrogenase (bGDH) (G2626-50MG; Sigma), which was monitored by continuous increase in absorbance at 340 nm using a Cary4000 UV-visible spectrophotometer. The assays were performed at room temperature in 20 mM Hepes pH 7.5, 100 mM KCl buffer. NAD^+ and bGDH concentrations were kept fixed at 2 mM and 1.7 μM, respectively, in the assays. Linear correlation between the initial rate of reaction and MccF enzyme concentration, at 500 μM ESA substrate concentration confirmed that the coupling enzymatic reaction was not rate limiting. MccF wild-type enzyme and W186F, R246A, N220A, and K247A mutants were assayed at 150 nM enzyme concentration. S118A, W186A, and N220A/K247A mutants were assayed at 750 nM enzyme concentration. Baseline absorbance was observed for 1 min before the reactions were initiated by the addition of enzyme.

Kinetics for the cleavage of DSA by MccF was determined by discontinuous HPLC separation of the reactant DSA and product sulfamoyl adenosine (SA). MccF wild-type enzyme and N220A mutant were assayed at 50 nM enzyme concentration. Seventy-five microliter enzymatic reactions were quenched by the addition of equal volumes of 4% formic acid and heating at 80 °C for 2 min. HPLC separation was performed on an analytical scale C18 column (Vydac; 5 μm particle size, 4.6 × 250 mm), monitored at 254 nm wavelength. One hundred microliters of the quenched reaction was injected to the C18 column and chromatography performed using 2% acetonitrile as buffer A and 80% acetonitrile as buffer B on an Agilent 1260 HPLC system. The elution gradient profile was as follows: wash with 5 mL of buffer A, elute with a continuous linear gradient to buffer B across 10 mL volume, wash with 5 mL buffer B, reduce acetonitrile concentration to 2% using a linear concentration gradient across 4 mL volume, reequilibrate with 6 mL buffer A. The flow rate was 1 mL/ min throughout the procedure. Different amounts of DSA without the addition of the enzyme were diluted into the reaction buffer and quenched and heated as above were injected, and a standard curve of the moles of reactant versus the area under the elution peak was determined. As the extinction coefficient of DSA and SA can be assumed to be the same at 254-nm wavelength, this standard curve was used to determine the number of moles of product formed in the subsequent enzymatic reaction time points. Measurements of the enzymatic rates were within the linear range of substrate turnover with respect to time, which was confirmed by the linear correlation between the measured initial rates and enzyme concentration across four different enzyme concentrations for each substrate concentration used. All data points were collected in triplicate and kinetic parameters determined by fitting the data to the Michaelis–Menten equation. Steady-state kinetic parameters for DSA hydrolysis by the N220A and K247A mutant enzymes were determined in an identical manner.

Hydrolysis of phenylalanine sulfamoyl adenylate (FSA) by MccF N220L/K247L was monitored in a manner identical to the kinetics determination of DSA hydrolysis by wild-type MccF. FSA (135 μM) was incubated with 450 nM of MccF N220L/K247L enzyme at room temperature in 20 mM Hepes, pH 7.5 buffer. Enzyme dilutions were made in 20 mM Hepes 100 mM KCl, pH 7.5 buffer. Reactions were initiated by the addition of enzyme. Aliquots from the reaction mixture were taken at different time points, quenched, and substrate and products were separated by HPLC. Substrate and product peak elution fractions were collected, lyophilized, dissolved in water, and analyzed by electrospray ionization mass spectrometry to confirm the identity of the substrate and product chemical species. A calibration curve between number of moles of substrate and area under the substrate peak (without the addition of the enzyme) was generated and used to calculate the amount of substrate consumed at different time points during the course of the enzyme reaction.

1. Otwinowski Z, et al. (2003) Multiparametric Scaling of Diffraction Intensities. *Acta Crystallogr A Found Crystallgr* 59:228–234.
2. Grosse-Kunstleve RW, Adams PD (2003) Substructure search procedures for macromolecular structures. *Acta Crystallogr D Biol Crystallogr* 59:1966–1973.
3. Terwilliger TC, et al. (2008) Iterative model building, structure refinement and density modification with the PHENIX AutoBuild wizard. *Acta Crystallogr D Biol Crystallogr* 64:61–69.
4. Emsley P, Cowtan K (2004) Coot: model-building tools for molecular graphics. *Acta Crystallogr D Biol Crystallogr* 60:2126–2132.
5. Murshudov GN, Vagin AA, Dodson EJ (1997) Refinement of macromolecular structures by the maximum-likelihood method. *Acta Crystallogr D Biol Crystallogr* 53:240–255.
6. Kleywegt GJ, Brunger AT (1996) Checking your imagination: Applications of the free R value. *Structure* 4:897–904.
7. Laskowski RA, et al. (1996) AQUA and PROCHECK-NMR: Programs for checking the quality of protein structures solved by NMR. *J Biomol NMR* 8:477–486.

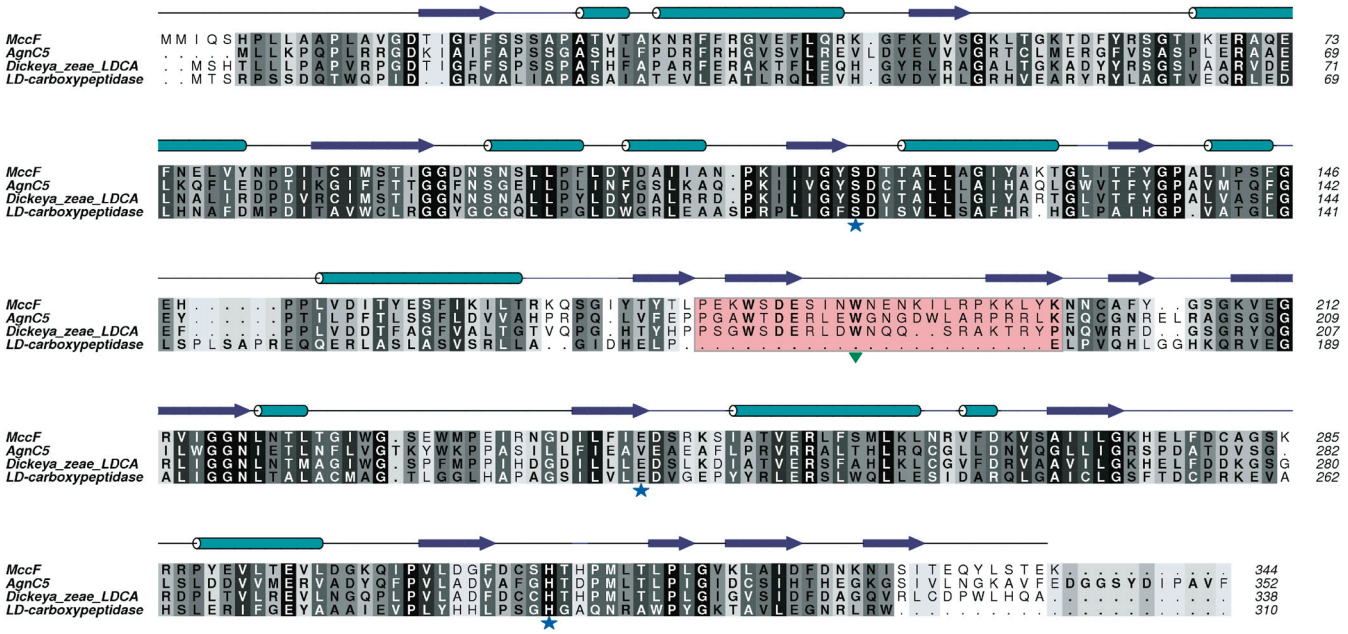

Fig. S1. Sequence alignment of MccF with an MccF homolog from the agrocin 84 biosynthetic gene cluster (AgnC5), hypothetical MccF homolog from *Dickeya zeae*, and *Pseudomonas aeruginosa* LD-carboxypeptidase. The catalytic triad residues are marked by star; the P1 site tryptophan residue is marked by arrowhead.

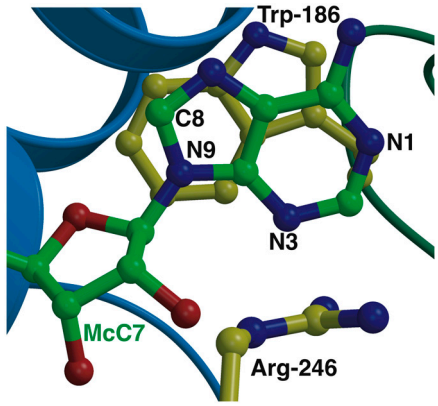

Fig. S2. Active site view of the cocrystal structure of Ser118Ala MccF with substrate McC7, illustrating the stacking interactions between Trp186 and the adenine ring of McC7. The N1 and N3 of the adenine, which have the greatest negative potential, are positioned furthest away from the six-membered ring of the indole side chain (which would bear the greatest negative potential). In addition, the positive potential bearing C8 and N9 positions of the adenine are stacked nearest to the six-membered ring. The electronegative N3 is also positioned near the basic guanidine side chain of Arg246. The two ring systems are postulated to align so as to minimize the electrostatic repulsion between the two heterocyclic *p*-electron systems. Enzyme side-chain residue carbon atoms are colored in yellow; McC7 carbon atoms are in green.

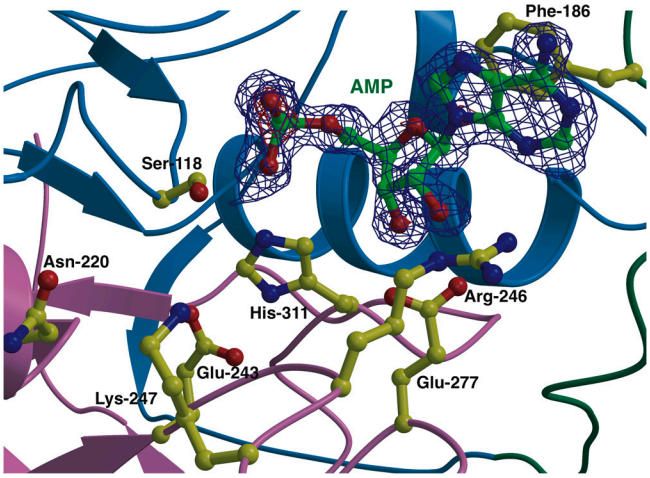

Fig. S3. Active site view of the cocrystal structure of Trp186Phe MccF with AMP. Enzyme side-chain residue carbon atoms are colored in yellow; AMP carbon atoms are colored in green. Superimposed is a difference Fourier electron density map (contoured at 2.7σ over background in blue) calculated with coefficients $|F_{obs}| - |F_{calc}|$ and phases from the final refined model with the coordinates of AMP deleted prior to one round of refinement. MccF N-terminal domain is colored blue, C-terminal domain is colored pink, and the catalytic loop is colored green as in Fig. 2*A*.

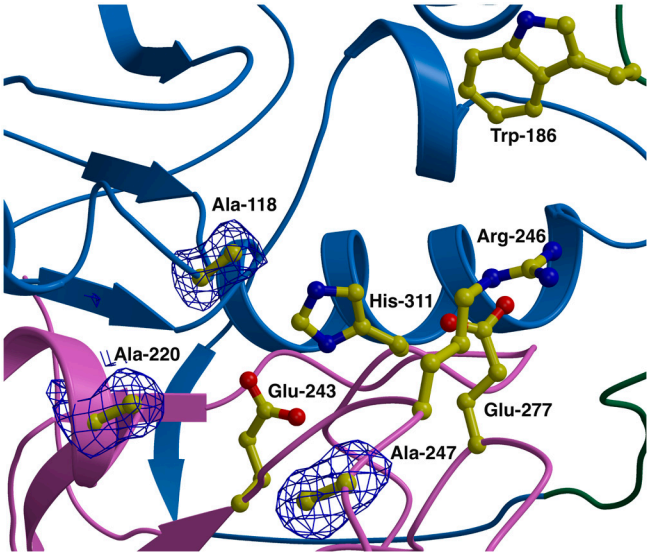

Fig. S4. Active site view of Ser118Ala/Asn220Ala/Lys247Ala MccF. Enzyme side-chain residue carbon atoms are colored in yellow. Superimposed is a difference Fourier electron density map (contoured at 2.7σ over background in blue) calculated with coefficients $|F_{obs}| - |F_{calc}|$ and phases from the final refined model with the coordinates of the side chains of Ala-118, Ala-220, and Ala-247 deleted prior to one round of refinement. MccF N-terminal domain is colored blue, C-terminal domain is colored pink, and the catalytic loop is colored green as in Fig. 2*A*.

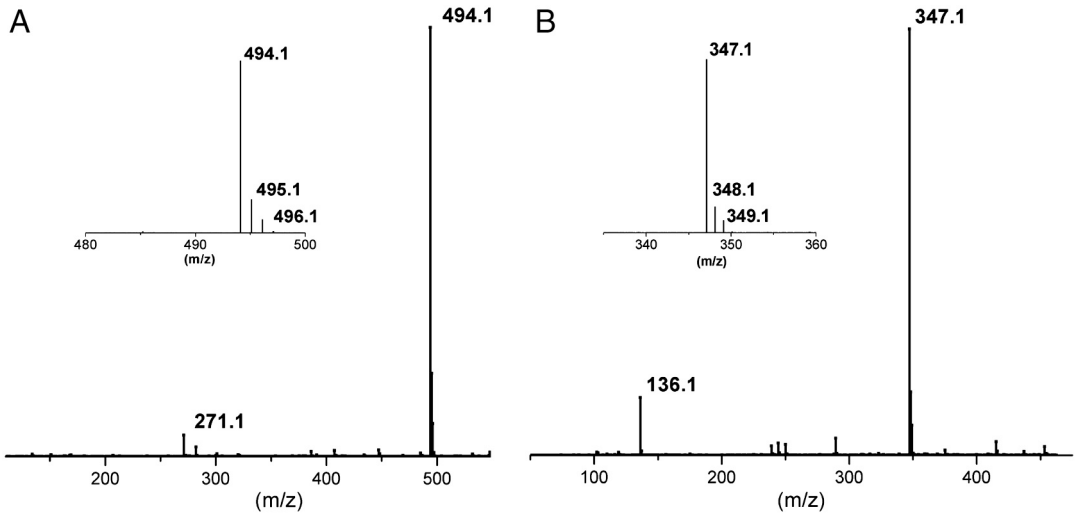

Fig. S5. Electrospray ionization (ESI) mass spectrum of the substrate and product peaks for phenylalanyl sulfamoyl adenosine (FSA) cleavage by MccF Asn220-Leu/Lys247Leu double mutant enzyme. (*A*) ESI spectra of substrate FSA peak. Inset shows the monoisotopic masses of the major peak corresponding to FSA. (*B*) ESI spectra of product sulfamoyl adenosine (SA) peak. Inset shows the monoisotopic masses of the major peak corresponding to SA.

Table S1. Data collection, phasing, and refinement statistics

	MccF (native)	Ser118Ala	MccF-ESA	MccF-DSA	MccF-McC7
Data collection					
Cell dimensions					
a, b, c (Å), β(°)	54.4, 85.9, 73,1 101.2	54.5, 85.8, 73.2 101.2	54.5, 85.9, 73.1 101.2	54.4, 85.7, 72.9 101.3	54.3, 85.7, 72.9 101.3
Resolution,* Å	50-1.2 (1.24-1.2)	50-1.5 (1.55-1.5)	50-1.35 (1.4-1.35)	50-1.5 (1.55-1.5)	50-1.3 (1.35-1.3)
Total reflections	1,470,584	488,868	538,837	594,715	680,252
Unique reflections	202,577	105,193	142,589	99,681	156,612
R_{sym}, %	6.8 (35.2)	6.9 (12.1)	4.5 (14.5)	5.8 (24.4)	5.0 (28.2)
$I/\sigma(I)$	38.7 (3.9)	46.3 (19.2)	39.6 (9.5)	27.9 (5.4)	29.8 (4.5)
Completeness, %	98.9 (93.8)	99.7 (99.8)	98.2 (96.2)	95.6 (85.0)	97.2 (93.8)
Redundancy	7.3 (5.8)	4.6 (4.6)	3.8 (3.6)	6.0 (5.3)	4.4 (4.1)
Refinement					
Resolution, Å	25-1.2	25-1.5	25-1.3	25-1.5	25-1.3
No. reflections	192,327	99,890	149,510	94,666	148,363
R_{work}/R_{free} †	18.3/20.1	17.7/19.8	17.9/19.7	17.9/20.2	17.4/18.6
No. of atoms					
Protein	5,313	5,188	5,261	5,261	5,277
Ligand	—	—	64	62	70
Water	961	981	957	864	978
B factors					
Protein	10.8	11.1	9.9	11.9	9.0
Ligand	—	—	22.5	20.5	14.2
Water	27.4	27.9	27.6	30.2	26.5
rmsd					
Bond lengths, Å	0.005	0.006	0.005	0.006	0.005
Bond angles, °	0.97	0.984	0.987	0.986	1.000

*Highest resolution shell is shown in parenthesis.

†R factor $= \Sigma(|F_{obs}| - k|F_{calc}|)/\Sigma|F_{obs}|$ and R free is the R value for a test set of reflections consisting of a random 5% of the diffraction data not used in refinement.